Published in final edited form as:
Circulation. 2009 January 20; 119(2): 261–268. doi:10.1161/CIRCULATIONAHA.108.799536.

DISRUPTION OF STRIATED PREFERENTIALLY EXPRESSED GENE LOCUS LEADS TO DILATED CARDIOMYOPATHY IN MICE

Xiaoli Liu, MD, PhD*, **Tripurasundari Ramjiganesh, PhD***, **Yen-Hsu Chen, MD, PhD**, **Su Wol Chung, PhD**, **Sean Hall, PhD**, **Scott L. Schissel, MD, PhD**, **Robert F. Padera Jr., MD, PhD**, **Ronglih Liao, PhD**, **Kate G. Ackerman, MD**, **Jan Kajstura, PhD**, **Annarosa Leri, MD**, **Piero Anversa, MD**, **Shaw-Fang Yet, PhD**, **Matthew D Layne, PhD**, and **Mark A Perrella, MD**

From Pulmonary and Critical Care Medicine, Brigham and Women's Hospital, 75 Francis St., Boston, MA 02115, and Harvard Medical School, Boston, MA, 02115 (X.L., T.R., S.W.C., S.H., S.L.S., M.A.P.), Newborn Medicine, Brigham and Women–s Hospital (M.A.P.), Division of Infectious Diseases, Department of Internal Medicine, Kaohsiung Medical University, 100 Shih-Chuan 1st Road, Kaohsiung, Taiwan, 807 (Y.-H.C.), School of Biological Science and Technology, College of Natural Sciences, University of Ulsan, San 29, Muger 2-dong, Ulsan, 680-749, South Korea (S.W.C.), Department of Pathology, Brigham and Women's Hospital, and Division of Health Sciences and Technology, Harvard-MIT (R.F.P.), Department of Anesthesia (J.K., A.L., P.A.) and Cardiovascular Division, Brigham and Women's Hospital and Harvard Medical School (R.L., J.K., A.L., P.A.), Department of Pediatrics, University of Rochester, 601 Elmwood Avenue, Rochester, NY 14642 (K.G.A.), Cardiovascular and Blood Medical Research Center, National Health Research Institutes, Zhunan Town, Miaoli County 35053, Taiwan (S.-F.Y.), Boston University School of Medicine, Department of Biochemistry, 715 Albany St. Boston, MA 02118 (M.D.L.).

Abstract

Background—The striated preferentially expressed gene (Speg) generates four different isoforms through alternative promoter use and tissue specific splicing. Depending on the cell type, Speg isoforms may serve as markers of striated or smooth muscle differentiation.

Correspondence to Mark A. Perrella, Division of Pulmonary and Critical Care Medicine, Brigham and Women's Hospital, 75 Francis Street, Boston, MA 02115. Phone: (617) 732-6809, Fax: (617) 582-6148, Email: mperrella@rics.bwh.harvard.edu.
*These authors contributed equally to this study.

Author Disclosures
Xiaoli Liu: No disclosures
Tripurasundari Ramjiganesh: No disclosures
Yen-Hsu Chen: No disclosures
Su Wol Chung: No disclosures
Sean Hall: No disclosures
Scott L. Schissel: No disclosures
Robert F. Padera: No disclosures
Ronglih Liao: No disclosures
Kate G. Ackerman: No disclosures
Jan Kajstura: No disclosures
Annarosa Leri: No disclosures
Piero Anversa: No disclosures
Shaw-Fang Yet: No disclosures
Matthew D. Layne: No disclosures
Mark A. Perrella: Research Grant: HL65639 (completed), March of Dimes Birth Defect Foundation (completed), Amount: >=$10,000

Journal Subject Heads: [130] Animal models of human disease, [108] Other myocardial biology

Methods and Results—To elucidate function of Speg gene isoforms, we disrupted the Speg gene locus in mice by replacing common exons 8, 9, and 10 with a lacZ gene. β-galactosidase activity was detected in cardiomyocytes of the developing heart, starting at day 11.5 days post-coitum (dpc). β-galactosidase activity in other cell types, including vascular smooth muscle cells, did not begin until 18.5 dpc. In the developing heart, protein expression of only Spegα and Spegβ isoforms was present in cardiomyocytes. Homozygous Speg mutant hearts began to enlarge by 16.5 dpc, and by 18.5 dpc demonstrated dilation of right and left atria and ventricles. These cardiac abnormalities in the absence of Speg were associated with a cellular hypertrophic response, myofibril degeneration, and a marked decrease in cardiac function. Moreover, Speg mutant mice exhibited significant neonatal mortality, with increased death occurring by 2 days after birth.

Conclusions—These findings demonstrate that mutation of the Speg locus leads to cardiac dysfunction and a phenotype consistent with a dilated cardiomyopathy.

Keywords

dilated cardiomyopathy; hypertrophy; myofibril; gene disruption

Introduction

Myosin light chain kinases (MLCK) are a family of proteins that are important for myocyte function, including structure and regulation of the actin-based cytoskeleton [1,2]. One member of this family, striated preferentially expressed gene (Speg), has isoforms in both striated and smooth muscle cells [3]. The Speg locus contains two transcriptional start sites, and through alternative promoter use and splicing in a tissue specific manner, generates four different isoforms [3]. Spegα and Spegβ are expressed in striated muscle (cardiac and skeletal), aortic preferentially expressed gene (Apeg-1) is expressed in smooth muscle (predominantly vascular), and brain preferentially expressed gene (Bpeg) is expressed in the brain and aorta [3–5]. Spegα and Spegβ share homology with MLCK family members. Specifically, the Speg isoforms, along with obscurin-MLCK, are unique members of the MLCK family as they contain two tandemly-arranged serine/threonine kinase (MLCK) domains [2]. Beyond the MLCK domains, Spegα and Spegβ also contain immunoglobulin and fibronectin domains that are characteristic of the MLCK family of proteins. Prior investigations in our laboratory revealed that Spegα and Spegβ are sensitive markers of striated muscle differentiation, and that Speg colocalizes with desmin in the sarcomeric Z disc [3]. However, the functional significance of Speg isoforms is yet to be elucidated.

In contrast to smooth muscle cells, striated muscle cells of both cardiac and skeletal origin undergo terminal differentiation shortly after birth in mammals, with the majority of these cells not retaining the ability to proliferate or regenerate after injury [6,7]. It has been shown that myocardial regeneration occurs following injury, due to the presence of cardiac progenitor cells, and this regeneration occurs predominantly in regions of the heart with a viable myocardium, outside of the infarcted area [8]. Thus, the ability to regenerate myocytes at regions of injury, and the therapeutic potential of progenitor cells [8,9], has been an intense area of investigation in the field of cardiovascular medicine, as heart failure due to myocardial injury and death remains a difficult and deadly problem for millions of Americans [10].

For cardiomyocytes to function appropriately, contractile forces generated in the sarcomere are transmitted to the extracellular matrix. If this process does not occur appropriately, cardiac remodeling of either a hypertrophic or dilated phenotype takes place. Hypertrophic cardiomyopathy (HCM) results in little or no increase in cardiac chamber volume, but thickening of the ventricular wall. In contrast, dilated cardiomyopathy (DCM) results in an increase in cardiac chamber volume and thinning of the ventricular wall [11]. It has been

suggested that familial forms of cardiomyopathy may result from alterations in different subsets of genes, for instance sarcomeric gene mutations (hypertrophic) versus cytoskeletal, contractile, and calcium regulatory gene mutations (dilated) [11,12]. However, this is not totally inclusive, as approximately 10% of cases of familial DCM may be due to mutations in sarcomere protein genes [13].

To study the potential importance of the Speg gene locus in cardiovascular biology, we removed exons 8, 9 and 10 of the Speg locus by targeted deletion. This mutation disrupted all of the Speg isoforms. Mice homozygous for this mutation died in the immediate neonatal period, and demonstrated a DCM with evidence of cellular hypertrophy, myofibril degeneration, and cardiac dysfunction. Spegα and Spegβ proteins were the only isoforms detected during this developmental period in the heart. This study demonstrates the importance of the Speg proteins for mouse cardiac development and survival.

Methods

Detailed methods are described in the Expanded Methods in the Data Supplement, available online at http://circ.ahajournals.org.

Generation of Speg Mutant Mice

The cloning strategy for generation of the Speg targeting construct, Southern blotting, and genotyping are described in detail in the Data Supplement.

Myofibril Extraction and Western Blotting

The myofibril fraction from 18.5 dpc hearts was extracted as described [14]. For more details see the Data Supplement.

Echocardiography

A Vevo 770 high-resolution microultrasound system and a 40-MHz probe (Visualsonics, Toronto, ON) were used for transthoracic echocardiography on non-anesthetized 18.5 dpc animals, as described [15].

Cardiac Weight Index

At 18.5 dpc, the embryos were harvested and their hearts removed. Cardiac weight index was calculated as heart wet weight (mg) divided by total body weight (g).

Myocyte size, number, and assessment of apoptosis

These cellular parameters were obtained as described [16,17]. For more details see the Data Supplement.

Two-dimensional Gel Electrophoresis and Western Blotting

Protein from 18.5 dpc hearts was extracted as described [14]. Electrophoresis and Western blotting were performed by Kendrick Laboratories Inc., Madison, WI, as described in the Data Supplement.

Isoelectric Focusing (IEF)

Heart tissue harvested from 16.5 dpc hearts. Electrophoresis on an IEF gel (pH 3~7, Invitrogen) and Western blotting were performed as described in the Data Supplement.

Statistical Analysis

One-way analysis of variance was used to determine differences between parameters of wild type (+/+) and homozygous (−/−) embryos/neonates. Scheffe F test was used as a post-hoc test and differences were considered significant at $P<0.05$.

The authors had full access to the data and take responsibility for its integrity. All authors have read and agree to the manuscript as written.

Results

Targeted Disruption of Speg Gene Locus

To generate Speg mutant mice, a targeting vector was constructed to replace exons 8, 9, and 10 of the Speg gene locus by a nuclear localized lacZ gene (Figure IA of online Data Supplement). Southern blot analyses (supplemental Figure IB) revealed that the 5'-probe hybridized to a 7 kb fragment in wild type mice (+/+, left lane), a 4 kb fragment in homozygous mutant mice (−/−, right lane), or both fragments in heterozygous mice (+/−, middle lane).

The Speg gene locus contains two transcription start sites (supplemental Figure IA, ↱), and through alternative splicing in a tissue specific manner generates four different isoforms, namely Spegβ, Spegα, Bpeg and Apeg-1 with a transcript size of 11, 9, 4 and 1.4 kb respectively [3]. Spegβ and Bpeg are transcribed from the first promoter, and Spegα and Apeg-1 from the second promoter. Northern blot analysis was performed on RNA extracted from 18.5 dpc hearts of +/+, +/−, and −/− embryos. Figure 1A depicts the Speg isoforms and the location of specific probes for Northern analysis. Using a probe encompassing the Apeg-1 coding region (Figure 1B, left panel), we observed transcripts corresponding with Spegβ, Spegα, Bpeg, and Apeg-1 in +/+ and +/− embryos. Speg isoform levels were reduced in +/− compared with +/+ mice, and not detected in −/− embryos. Using the 5' Speg probe, we detected transcripts corresponding with Spegβ and Bpeg in +/+ and +/− embryos (Figure 1B, middle panel). Interestingly, as the mRNA levels for Spegβ and Bpeg decreased in +/− and −/− embryos, deletion of exons 8–10 resulted in splicing of exon 7 into the lacZ splice acceptor site, which produced a mutant 6.4 kb message (Figure 1B, middle panel asterisks). Using the 3' Speg probe, we detect transcripts corresponding with Spegα and Spegβ in +/+ embryos, and these transcript levels decreased in +/− and −/− embryos (Figure 1B, right panel). 18S hybridization verified equal RNA loading.

Western blot analysis was performed on myofibril fractions obtained from 18.5 dpc +/+, +/−, and −/− hearts. Blotting with an affinity purified Speg/Apeg-1 antibody [3] revealed ~250 kDa and ~350 kDa bands consistent with Spegα and Spegβ in +/+ and +/− hearts, but not in −/− hearts (Figure 1C). Even though mRNA for Apeg-1 and Bpeg was present in heart homogenates of +/+ and +/− mice, protein expression for Apeg-1 and Bpeg was not detected in myofibril fractions of 18.5 dpc hearts. These data demonstrate that the Speg isoforms present in cardiac myofibrils at this developmental time point are of Spegα and Spegβ origin. The non-specific (NS) band and reblotting with an antibody against desmin (Des) demonstrated equivalent protein loading.

LacZ Transgene Expression During Development in Heterozygous Speg Mutant Embryos

The gene targeting strategy effectively knocked in the bacterial lacZ reporter gene under the transcriptional control of Spegα/Apeg-1 promoter. We evaluated lacZ staining in the heterozygous embryos to determine the localization of Spegα/Apeg-1 promoter activity during development. At 11.5 dpc, lacZ staining was restricted to the heart (Figure 2A). Staining was evident in both right and left atria and future ventricles, but not the outflow tract (Figure 2B and Figure 2C). At 16.5 dpc, lacZ staining remained predominantly in the heart (Figure 2D),

and histological analysis revealed both atrial (Figure 2E) and ventricular (Figure 2F) staining in cardiomyocytes. At 16.5 dpc, there was no evidence of staining in the aortic arch or great vessels (Figure 2D). At 18.5 dpc, lacZ staining persisted in both right and left atria and ventricles of the heart (Figure 2G–H). Staining was apparent in the trachea (Figure 2G), but this staining was in the respiratory epithelium and not the airway smooth muscle cells (SMC) (data not shown). At 18.5 dpc, staining was seen for the first time in elastic arteries, including the aorta, carotid arteries, and pulmonary arteries (Figure 2I). Within the vessel wall, staining was evident in SMC, but not endothelial cells (EC), as seen in the pulmonary arteries (Figure 2J–K). However, no evidence of coronary artery staining was present at 18.5 dpc (Figure 2L), suggesting a lack of β-galactosidase activity in muscular arteries. Taken together, these data demonstrate that Speg isoform expression was predominantly in cardiomyocytes of both atria and ventricles from 11.5 through 16.5 dpc (consistent with the Spegα isoform), and expression outside the heart did not begin until 18.5 dpc in vascular SMC of elastic arteries (consistent with the Apeg-1 isoform), but not in muscular arteries including the coronary vessels.

Neonatal Death in Homozygous Speg Mutant Mice

$Speg^{+/-}$ mice on a 129Sv X C57BL/6 background were phenotypically normal and fertile, and were bred to generate $Speg^{-/-}$ mutant mice. Among 122 embryos genotyped at 15.5 dpc or earlier, there was a genotype distribution of 26% +/+, 53% +/−, and 21% −/− (Table 1), suggesting no remarkable early embryonic death. Analysis of genotypes at 18.5 dpc revealed a Mendelian distribution of 21% +/+, 58% +/−, and 21% −/− embryos. However, starting at day 2 postnatally, lethality increased dramatically in the $Speg^{-/-}$ neonates. By 21 days postpartum, of the 360 offspring from heterozygous breeding there were only 2% viable $Speg^{-/-}$ mice (Table 1). These data indicate that $Speg^{-/-}$ mice survive embryonic development, but the majority of mutant mice die in the early postnatal period. After breeding the 129Sv X C57BL/6 $Speg^{+/-}$ mice to a pure C57BL/6 background (9 generations), no viable $Speg^{-/-}$ mice were observed postnatally. In contrast, the $Speg^{+/-}$ mice appear normal with no evidence of lethality in adult mice.

Cardiac Abnormalities in $Speg^{-/-}$ Embryos

Overall size and body weight were not different between $Speg^{+/+}$ (1.36 ± 0.053 g), $Speg^{+/-}$ (1.30 ± 0.038 g), and $Speg^{-/-}$ (1.21 ± 0.025 g, P=0.1316 with a minimum of n=8 per group) pups at 18.5 dpc. The most obvious phenotype in the $Speg^{-/-}$ embryos was enlargement of the heart. By 16.5 dpc, the $Speg^{-/-}$ embryos began to show evidence of heart dilatation (Figure 3A, top right panel) compared with $Speg^{+/+}$ embryos (Figure 3A, top left panel). However, by 18.5 dpc, $Speg^{-/-}$ embryos revealed a more dramatic dilatation of the heart, with involvement of both right and left atrial and ventricular chambers (Figure 3A, bottom right panel). The ventricular walls appeared thinner in Speg mutant hearts, and we found no evidence of septal defects between the right and left side of the heart, and no valvular abnormalities. The absolute cardiac weights were 7.7±0.4 mg for $Speg^{+/+}$ mice (n=15), and 10.3±0.6 mg for $Speg^{-/-}$ mice (n=12, P<0.05). To further determine whether there was evidence of cardiac hypertrophy, cardiac weight index (CWI) and morphologic analysis of cardiomyocytes were assessed in $Speg^{+/+}$ and $Speg^{-/-}$ embryos. $Speg^{-/-}$ embryos revealed a significant increase in CWI compared with $Speg^{+/+}$ embryos (P<0.05, Figure 3B). In addition, differences were detected in the structural organization of the myocardium in $Speg^{-/-}$ compared with and $Speg^{+/+}$ mice at E18.5 (Figure 4A). The heart of $Speg^{-/-}$ mice were characterized by a reduced density of myocyte nuclei per unit area of tissue, suggesting that cellular hypertrophy and/or cell death contributed to the cardiac phenotype. However, measurements of apoptosis indicated that myocyte death was present in comparable proportions in both groups of animals (1.21 ± 0.37 versus 1.18 ± 0.39 apoptotic cells/1000 cells in $Speg^{+/+}$ and $Speg^{-/-}$ hearts, n=5 and 6 mice respectively). Therefore, the volume and number of maturing cardiomyocytes were determined quantitatively. In comparison with $Speg^{+/+}$, the myocardium of $Speg^{-/-}$ mice was composed

of myocytes which were 20% larger while their number per mm^3 of tissue was reduced by 17% (Figure 4B). These observations suggest that mutation of the Speg gene locus affected the generation of parenchymal cells during development, evoking a cellular hypertrophic response

$Speg^{-/-}$ neonates allowed to spontaneously breath after delivery at 18.5 dpc had significantly smaller lungs than $Speg^{+/+}$ neonates (Figure 3A, bottom panels), although lung weight was comparable (data not shown). $Speg^{-/-}$ neonates spontaneously breathing on day 1 after birth, when comparably inflated, revealed lung architecture not remarkably different from $Speg^{+/+}$ neonates (supplemental Figure II). Reduction in lung size was directly related to an increase in heart size, resulting in compression of the lungs. Examination of other organs did not show obvious abnormalities to account for the neonatal lethality, and no gross abnormalities in the vasculature (with normal anatomical positions of the great vessels) or skeletal muscle (including muscularization of the diaphragm, data not shown) at birth.

Further histologic analysis of the $Speg^{+/+}$ and $Speg^{-/-}$ hearts was performed. Figure 5A depicts a section from the epicardial through the myocardial layers (not including the endocardium) of the left ventricular free wall of a $Speg^{+/+}$ pup, 1 day after birth. In contrast, an analogous section from a $Speg^{-/-}$ heart is shown in Figure 5B. The epicardial through the myocardial layers of the left ventricular free wall was thinner in the $Speg^{-/-}$ heart, with the endocardial layer present in this section, as demarcated by the trabeculae (Figure 5B). In addition, there was evidence of dilated subepicardial vessels in the $Speg^{-/-}$ hearts compared with $Speg^{+/+}$ hearts (arrows). Higher power images of cardiomyocytes from the myocardial layer of $Speg^{-/-}$ hearts revealed evidence of vacuoles and less well developed striations (Figure 5D) compared with $Speg^{+/+}$ hearts (Figure 5C). To further assess for ultrastructural changes, hearts from C57BL/6 pure background embryos (18.5 dpc) were harvested for transmission electron microscopy analyses. $Speg^{+/+}$ hearts showed a tightly packed sarcomere with normal alignment of myofibrils, intact Z discs, and clearly defined intercalated discs (Figure 5E). However, $Speg^{-/-}$ hearts appeared dramatically different, with evidence of myofibril degeneration and sarcomere fragmentation (Figure 5F). To assess the functional status of Speg mutant hearts, we performed echocardiograms on 18.5 dpc embryos. There was a marked reduction in cardiac function (left ventricular fractional shortening and ejection fraction) in $Speg^{-/-}$ hearts compared with $Speg^{+/+}$ hearts ($P<0.05$, Figure 5G). $Speg^{+/+}$ mouse hearts had fractional shortenings of 40 ± 2 % and ejection fractions of 74 ± 2 %, while $Speg^{-/-}$ mouse hearts had fractional shortenings and ejection fractions of 10 ± 1 % and 23 ± 3 % respectively. These data suggest that the structural integrity of the heart is remarkably abnormal in the $Speg^{-/-}$ embryos, with marked cardiac dysfunction.

Altered Phosphorylation of Tropomyosin in Speg Mutant Mice

To further understand why Speg mutant mice (with absence of the unique kinase domains [3]) develop a DCM, we performed two-dimensional gel electrophoresis on protein extracts from 18.5 dpc hearts of $Speg^{+/+}$ and $Speg^{-/-}$ mice, followed by anti-phosphoserine/anti-phosphothreonine Western blotting. Differentially phosphorylated proteins were identified by mass spectrometry analysis. Figure 6A revealed 3 spots (identified by arrows) that were present in $Speg^{+/+}$ hearts, but not $Speg^{-/-}$ hearts. These spots were submitted for mass spectrometry analysis to identify the differentially phosphorylated proteins. Tropomyosin (TM) proteins were in all of the spots, with TM α-1 chain (α-TM or TM 1) predominating. Tropomyosin α-4 chain (TM 4) was also prominent in one of the spots along with α-TM (supplemental Table I), and there was less evidence for the contribution of TM β chain (β-TM or TM 2). For further delineation of the phosphorylation status of tropomyosin, we ran protein extracts from 16.5 dpc $Speg^{+/+}$, $Speg^{+/-}$, and $Speg^{-/-}$ mouse hearts on an isoelectric focusing (IEF) gel, followed by Western blotting of the transferred protein using an anti-tropomyosin antibody (Figure 6B). Protein extracts from the hearts of $Speg^{-/-}$ embryos demonstrated a different isoelectric focus

(Figure 6B, lanes 3 and 7 lower bands) compared with hearts of $Speg^{+/+}$ and $Speg^{+/-}$ embryos. Moreover, when protein from $Speg^{+/+}$ hearts was treated with phosphatase, the migration pattern of tropomyosin shifted down, consistent with that of $Speg^{-/-}$ hearts. While there was a difference in phosphorylation, the overall tropomyosin content by conventional Western blotting was not different between $Speg^{+/+}$ and $Speg^{-/-}$ hearts (Figure 6C). These data suggest a decreased level of phosphorylated tropomyosin in $Speg^{-/-}$ hearts.

Discussion

Heart growth during organogenesis occurs principally through the proliferation of cardiomyocytes. After birth, excluding progenitor cells, cardiomyocytes withdraw from the cell cycle and further growth occurs by hypertrophy [18]. A hypertrophic stimulus may progress to a DCM, in part, by the activation of cell death pathways, including apoptosis [19]. However, in $Speg^{-/-}$ mice, there is no difference in myocyte apoptosis compared with $Speg^{+/+}$ mice, and mutation of the Speg gene locus affected the generation of parenchymal cells evoking a cellular hypertrophic response.

DCM is the most common form of primary cardiac muscle disease, with an estimated prevalence in the United States of 36.5 per 100,000 people [20]. Furthermore, DCM is not only a disease of adults, as DCM is one of the most common non-structural fetal heart abnormalities [21,22]. DCMs have been linked to gene mutations in cytoskeletal proteins; for example dystrophin, desmin, and cardiac muscle LIM protein [13,23–28]. However, gene mutations in sarcomere proteins (such as cardiac β-myosin heavy chain, troponin T, α-tropomyosin, cardiac actin, and cardiac myosin-binding protein-C) have also been associated with dilated forms of cardiomyophathy, and may account for a subset of these cases [13,28–31]. Beyond the identification of specific genes, disease loci for familial DCM have been identified on various chromosomes, including regions on chromosome 2q (2q14-q22, 2q31, and 2q35) [12]. These chromosomal loci harbor potential causative genes, and interestingly the Speg/Apeg-1 locus, mapped to chromosome 2q34 [5], lies in close proximity to the 2q35 locus of desmin [24].

In evaluating the $Speg^{+/-}$ embryos during development, the expression pattern of the lacZ transgene, driven by the Spega/Apeg-1 promoter, was localized exclusively in the heart (cardiomyocytes) throughout the first 16.5 dpc (Figure 2), a point in time that hearts in $Speg^{-/-}$ mice had already begun to enlarge (Figure 3A). At 18.5 dpc cardiac expression remained robust, while vascular expression of the lacZ transgene first became evident in elastic arteries, but not in the muscular coronary arteries. Moreover, structure of the pulmonary arteries and aorta did not appear structurally abnormal in the mutant mice. These data suggest that developmental abnormalities in mutant embryos result from the loss of Spegα and Spegβ expression in cardiomyocytes. However, future studies will need to further assess any vascular contribution to the phenotype, particularly in the setting of a pathophysiologic stress in $Speg^{+/-}$ mice.

The messages for all Speg isoforms are present in the mouse heart at day 18.5 (Figure 1); however, when assessing protein expression, only Spegα, and Spegβ are present in myofibrils. Northern blot analysis also demonstrated that as the mRNA levels for Spegβ decreased in heterozygous and homozygous mutant embryos, splicing of exon 7 into the lacZ splice acceptor site resulted in a mutant 6.4 kb message (Figure 1B). Since the heterozygous mice appear normal, with normal Mendelian ratio at birth and normal survival and fertility, we do not expect the lethal cardiac phenotype to be related to this transcript encoding a dominant negative protein.

Spegα and Spegβ share homology with MLCK family members. MLCK itself is a calcium/calmodulin-dependent protein kinase that phosphorylates a serine on the regulatory light chain

of myosin II [1]. Vertebrates have two muscle predominant MLCK genes: a skeletal/cardiac muscle MLCK gene, and a separate gene that through alternative promoter use gives rise to two smooth muscle MLCK genes and to telokin. Somlyo and colleagues reported a knockout of smooth muscle MLCK genes in mice [32], which led to death shortly after birth. Mutant hearts demonstrated irregular and dilated subepicardial vessels, and differences in the compact zone myocardial area compared with wild-type hearts [32]. Spegα and Spegβ, along with obscurin-MLCK, are unique members of the striated muscle MLCK family as they contain two tandemly-arranged serine/threonine kinase (MLCK) domains [2]. To our knowledge, the generation of the Speg mutant locus in this study is the first description of a tandem-kinase family member to be disrupted in mice.

In an effort to provide insight into a potential mechanism responsible for the DCM that develops in Speg mutant mice, we performed a proteomic screen using two-dimensional gel electrophoresis on protein extracts from 18.5 dpc hearts of $Speg^{-/-}$ mice compared with $Speg^{+/+}$ mice. Furthermore, due to the unique tandemly-arranged serine/threonine kinase domains in Spegα and Spegβ [2], we assessed differentially phosphorylated proteins by anti-phosphoserine/anti-phosphothreonine Western blotting, and then performed mass spectrometry analysis to specifically identify the altered proteins. Our analysis, as shown in Figure 6A, revealed that phosphorylated proteins present in $Speg^{+/+}$ mice, but absent in $Speg^{-/-}$ mice, include TM isoforms. The predominant isoform identified was α-TM, which is known to be phosphorylated at its penultimate Ser283 [33].

α-TM is one of the regulatory proteins in the thin filament of striated muscle, and it binds with actin to form the backbone of the thin filament [34]. Together with the troponin complex, α-TM and actin play a critical role in striated muscle contraction and relaxation [35]. Phosphorylation of Ser283 is known to enhance actin activated ATPase activity without altering calcium sensitivity [36]. Of the TM isoforms, phosphorylation is higher in the α-TM subunit, and the phosphorylation status decreases after development and into adulthood [33]. These data suggest a functional role for α-TM phosphorylation during muscle development. Interestingly, it has recently been shown that chronic activation of p38 mitogen activated protein kinase in transgenic mouse hearts is able to depress sarcomeric function in association with an increase in dephosphorylation of α-TM [37]. In our present study, phosphorylated isoforms of TM (particularly α) are absent in 18.5 dpc hearts of $Speg^{-/-}$ mice, in conjunction with a DCM leading to death. While a TM kinase was originally isolated and partially purified in chicken embryos [33], our present study suggests that Speg plays a role in TM phosphorylation during development. This alteration in α-TM phosphorylation, in the setting of a mutated Speg locus, may contribute to the development of DCM in $Speg^{-/-}$ mice. However, we cannot exclude the possibility that decreased α-TM phosphorylation may be a consequence, rather than a cause, of cardiac dysfunction. The DCM may be more related to structural consequences of a disruption in Speg, a protein known to colocalize with desmin in the sarcomeric Z disc [3]. The absence of Speg itself may alter the structural integrity and organization of the myofibril. Nevertheless, the present study demonstrates that Speg is important for cardiomyocyte development, and that disruption of the gene locus leads to DCM and neonatal death in mice.

Supplementary Material

Refer to Web version on PubMed Central for supplementary material.

Nonstandard abbreviations

Speg, striated preferentially expressed gene; Apeg, aortic preferentially expressed gene; Bpeg, brain preferentially expressed gene; +/+, wild type; +/−, heterozygous; −/−, homozygous;

DCM, dilated cardiomyopathy; dpc, day post-coitum; smc, smooth muscle cells; TM, tropomyosin.

Acknowledgments

The authors are grateful for the advice and helpful suggestions from Dr. Thomas Mariani; and the technical support of Darragh Cullen.

Sources of Funding

This work was supported by National Institutes of Health grants HL65639, HL60788, and GM53249 (to M.A. Perrella), a grant from the March of Dimes Birth Defects Foundation (to M.A. Perrella), and Harvard University-Kaohsiung Medical University Alliance and National Science Council (Taiwan) Grant NSC92-2314-B-037-028 (to Y.-H. Chen).

References

1. Kamm KE, Stull JT. Dedicated myosin light chain kinases with diverse cellular functions. J. Biol. Chem 2001;276:4527–4530. [PubMed: 11096123]
2. Sutter SB, Raeker MO, Borisov AB, Russell MW. Orthologous relationship of obscurin and Unc-89: phylogeny of a novel family of tandem myosin light chain kinases. Dev. Genes Evol 2004;214:352–359. [PubMed: 15185077]
3. Hsieh C-M, Fukumoto S, Layne MD, Maemura K, Charles H, Patel A, Perrella MA, Lee M-E. Striated muscle preferentially expressed genes alpha and beta are two serine/threonine protein kinases derived from the same gene as the aortic preferentially expressed gene-1. J. Biol. Chem 2000;275:36966–36973. [PubMed: 10973969]
4. Hsieh C-M, Yoshizumi M, Endege WO, Kho C-J, Jain MK, Kashiki S, de los Santos R, Lee W-S, Perrella MA, Lee M-E. APEG-1, a novel gene preferentially expressed in aortic smooth muscle cells, is down-regulated by vascular injury. J. Biol. Chem 1996;271:17354–17359. [PubMed: 8663449]
5. Hsieh C-M, Yet S-F, Layne MD, Watanabe M, Hong AM, Perrella MA, Lee M-E. Genomic cloning and promoter analysis of aortic preferentially expressed gene-1. Identification of a vascular smooth muscle-specific promoter mediated by an E box motif. J. Biol. Chem 1999;274:14344–14351. [PubMed: 10318857]
6. Soonpaa MH, Field LJ. Survey of studies examining mammalian cardiomyocyte DNA synthesis. Circ. Res 1998;83:15–26. [PubMed: 9670914]
7. Molkentin JD, Olson EN. Defining the regulatory networks for muscle development. Curr. Opin. Genet. Dev 1996;6:445–453. [PubMed: 8791524]
8. Leri A, Kajstura J, Anversa P. Cardiac stem cells and mechanisms of myocardial regeneration. Physiol. Rev 2005;85:1373–1416. [PubMed: 16183916]
9. Anversa P, Leri A, Rota M, Hosoda T, Bearzi C, Urbanek K, Kajstura J, Bolli R. Stem cells, myocardial regeneration, and methodological artifacts. Stem Cells 2007;25:589–601. [PubMed: 17124006]
10. Morita J, Seidman J, Seidman CE. Genetic causes of human heart failure. J. Clin. Invest 2005;115:518–526. [PubMed: 15765133]
11. Chien KR. Genomic circuits and the integrative biology of cardiac diseases. Nature 2000;407:227–232. [PubMed: 11001065]
12. Ahmad F, Seidman JG, Seidman CE. The genetic basis for cardiac remodeling. Annu. Rev. Genomics Hum. Genet 2005;6:185–216. [PubMed: 16124859]
13. Kamisago M, Sharma SD, DePalma SR, Solomon S, Sharma P, McDonough B, Smoot L, Mullen MP, Woolf PK, Wigle ED, Seidman JG, Seidman CE. Mutations in sarcomere protein genes as a cause of dilated cardiomyopathy. N. Engl. J. Med 2000;343:1688–1696. [PubMed: 11106718]
14. Zakhary DR, Moravec CS, Stewart RW, Bond M. Protein kinase A (PKA)-dependent troponin-I phosphorylation and PKA regulatory subunits are decreased in human dilated cardiomyopathy. Circulation 1999;99:505–510. [PubMed: 9927396]
15. Liao R, Jain M, Cui L, D'Agostino J, Aiello F, Luptak I, Ngoy S, Mortensen RM, Tian R. Cardiac-specific overexpression of GLUT1 prevents the development of heart failure attributable to pressure overload in mice. Circulation 2002;106:2125–2131. [PubMed: 12379584]

16. Anversa, P.; Olivetti, G. Cellular basis of physiological and pathological myocardial growth. New York: Oxford University Press; 2002.
17. Rota M, LeCapitaine N, Hosoda T, Boni A, De Angelis A, Padin-Iruegas ME, Esposito G, Vitale S, Urbanek K, Casarsa C, Giorgio M, Lüscher TF, Pelicci PG, Anversa P, Leri A, Kajstura J. Diabetes promotes cardiac stem cell aging and heart failure, which are prevented by deletion of the p66shc gene. Circ. Res 2006;99:42–52. [PubMed: 16763167]
18. Olson EN, Schneider MD. Sizing up the heart: Development redux in disease. Genes Dev 2003;17:1937–1956. [PubMed: 12893779]
19. Kang PM, Izumo S. Apoptosis in heart: Basic mechanisms and implications in cardiovascular diseases. Trends Mol. Med 2003;9:177–182. [PubMed: 12727144]
20. Michels VV, Moll PP, Miller FA, Tajik AJ, Chu JS, Driscoll DJ, Burnett JC, Rodeheffer RJ, Chesebro JH, Tazelaar HD. The frequency of familial dilated cardiomyopathy in a series of patients with idiopathic dilated cardiomyopathy. N. Engl. J. Med 1992;326:77–82. [PubMed: 1727235]
21. Burch M, Siddiqi SA, Celermajer DS, Scott C, Bull C, Deanfield JE. Dilated cardiomyopathy in children: Determinants of outcome. Br. Heart J 1994;72:246–250. [PubMed: 7946775]
22. Eronen M. Outcome of fetuses with heart disease diagnosed in utero. Arch. Dis. Child Fetal Neonatal Ed 1997;77:F41–F46. [PubMed: 9279182]
23. Towbin JA, Hejtmancik JF, Brink P, Gelb B, Zhu XM, Chamberlain JS, McCabe ER, Swift M. X-linked dilated cardiomyopathy. Molecular genetic evidence of linkage to the Duchenne muscular dystrophy (dystrophin) gene at the Xp21 locus. Circulation 1993;87:1854–1865. [PubMed: 8504498]
24. Goldfarb LG, Park KY, Cervenakova L, Gorokhova S, Lee HS, Vasconcelos O, Nagle JW, Semino-Mora C, Sivakumar K, Dalakas MC. Missense mutations in desmin associated with familial cardiac and skeletal myopathy. Nat. Genet 1998;19:402–403. [PubMed: 9697706]
25. Wang X, Osinska H, Dorn II GW, Nieman M, Lorenz JN, Gerdes AM, Wit S, Kimball T, Gulick J, Robbins J. Mouse model of desmin-related cardiomyopathy. Circulation 2001;103:2402–2407. [PubMed: 11352891]
26. Arber S, Hunter JJ, Ross J Jr, Hongo M, Sansig G, Borg J, Perriard JC, Chien KR, Caroni P. MLP-deficient mice exhibit a disruption of cardiac cytoarchitectural organization, dilated cardiomyopathy, and heart failure. Cell 1997;88:393–403. [PubMed: 9039266]
27. Chien KR. Genomic circuits and the integrative biology of cardiomyopathies. Eur. Heart J 2001;3:L3–L9.
28. Chu G, Haghighi K, Kranias EG. From mouse to man: Understanding heart failure through genetically altered mouse models. J. Cardiac Failure 2002;8:S432–S449.
29. Olson TM, Kishimoto NY, Whitby FG, Michels VV. Mutations that alter the surface charge of alpha-tropomyosin are associated with dilated cardiomyopathy. J. Mol. Cell. Cardiol 2001;33:723–732. [PubMed: 11273725]
30. Olson TM, Michels VV, Thibodeau SN, Tai Y-S, Keating MT. Actin mutations in dilated cardiomyopathy, a heritable form of heart failure. Science 1998;280:750–752. [PubMed: 9563954]
31. McConnell BK, Jones KA, Fatkin D, Arroyo LH, Lee RT, Aristizabal O, Turnbull DH, Georgakopoulos D, Kass D, Bond M, Niimura H, Schoen FJ, Conner D, Fischman DA, Seidman CE, Seidman JG. Dilated cardiomyopathy in homozygous myosin-binding protein-C mutant mice. J. Clin. Invest 1999;104:1235–1244. [PubMed: 10545522]
32. Somlyo AV, Wang H, Choudhury N, Khromov AS, Majesky M, Owens GK, Somlyo AP. Myosin light chain kinase knockout. J. Muscle Res. Cell Motil 2004;25:241–242. [PubMed: 15467390]
33. deBelle I, Mak AS. Isolation and characterization of tropomyosin kinase from chicken embryo. Biochimica et. Biophysica Acta 1987;925:17–26. [PubMed: 3593768]
34. Wolska BM, Wieczorek DF. The role of tropomyosin in the regulation of myocardial contraction and relaxation. Pflugers Arch 2003;116:1–8. [PubMed: 12690456]
35. Kobayashi T, Solaro RJ. Calcium, thin filaments, and the integrative biology of cardiac contractility. Annu. Rev. Physiol 2005;67:39–67. [PubMed: 15709952]
36. Heeley DH. Investigation of the effects of phosphorylation of rabbit striated muscle alpha-tropomyosin and rabbit skeletal muscle troponin-T. Eur. J. Biochem 1994;221:129–137. [PubMed: 8168502]

37. Vahebi S, Ota A, Li M, Warren CM, de Tombe PP, Wang Y, Solaro J. p38-MAPK induced dephosphorylation of α -tropomyosin is associated with depression of myocardial sarcomeric tension and ATPase activity. Circ. Res 2007;100:408–415. [PubMed: 17234967]

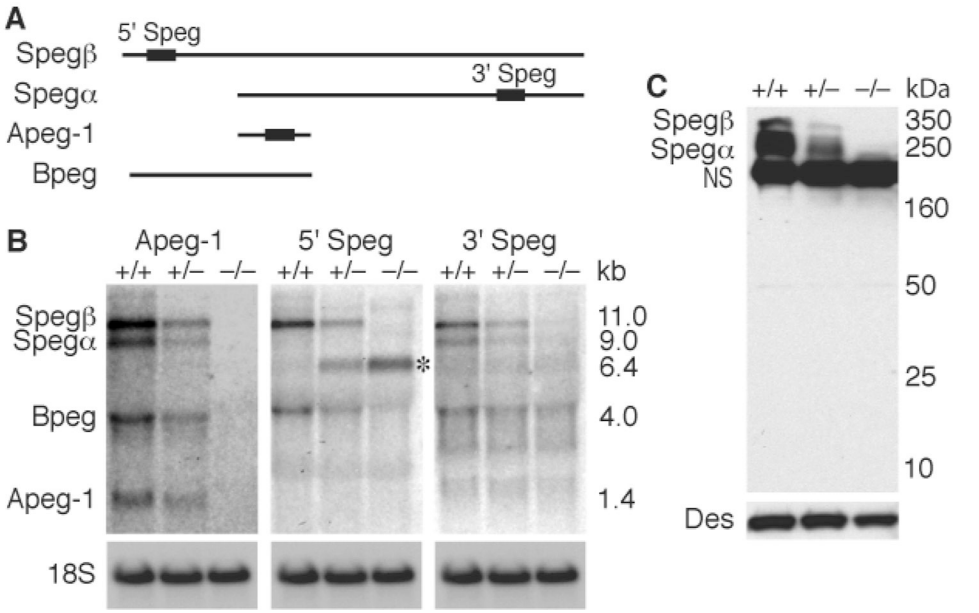

Figure 1.

Targeted disruption of the mouse Speg locus. (**A**) Schematic representation of Spegβ, Spegα, Apeg-1, and Bpeg isoforms, with location of 5' Speg, 3' Speg and Apeg-1 probes depicted by black rectangles. (**B**) Northern analysis of Spegβ, Spegα, Bpeg and Apeg-1 mRNA expression. RNA (10μg) extracted from 18.5 dpc wild type (+/+), heterozygous (+/−), and homozygous (−/−) mutant hearts were hybridized sequentially with probes for Apeg-1 (left panel), 5' Speg (middle panel), and 3' Speg (right panel) to assess message for the different Speg isoforms in the mouse hearts. The Northern blot was also hybridized with an 18S probe to assess RNA loading. * denotes the splice mutant band for Spegβ and Bpeg. (**C**) Myofibril protein was extracted from 18.5 dpc wild type (+/+), heterozygous (+/−), and homozygous (−/−) mutant hearts, and 10μg of protein was subjected to western blotting with an affinity purified Speg/Apeg-1 antibody, or an antibody to desmin (Des) to assess protein loading, as described in the materials and methods section. NS represents a non-specific band.

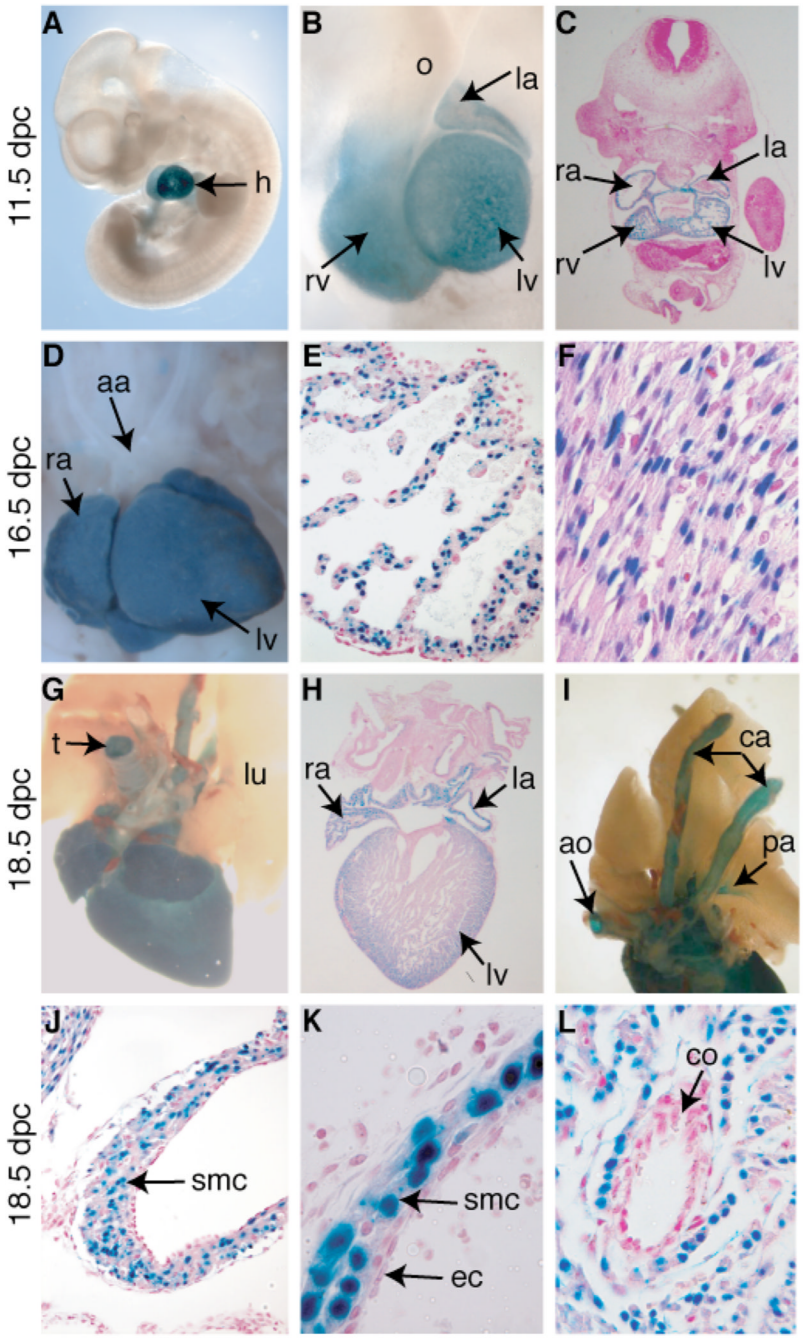

Figure 2.

Expression of the lacZ transgene by the Spegα/Apeg-1 promoter during development. Heterozygous (+/−) mutant embryos of age 11.5 (**A–C**), 16.5 (**D–F**), and 18.5 (**G–L**) dpc were isolated, fixed, and stained for β-galactosidase activity (blue). Whole mount staining was performed on intact embryos (**A**) or organs (**B, D, G, I**) of the thoracic cavity. Histological sections were counterstained with nuclear fast red (**C, E, F, H, J, K, L**). Heart (h); outflow tract (o); left atrium (la); right atrium (ra); left ventricle (lv); right ventricle (rv); aortic arch (aa); trachea (t); lung (lu); aorta (ao); carotid artery (ca); pulmonary artery (pa); smooth muscle cells (smc); endothelial cells (ec); coronary artery (co). Original magnifications X20 (**G, H, I**), X40 (**A, C**), X63 (**B, D**), X100 (**E, J, L**), and X200 (**F, K**).

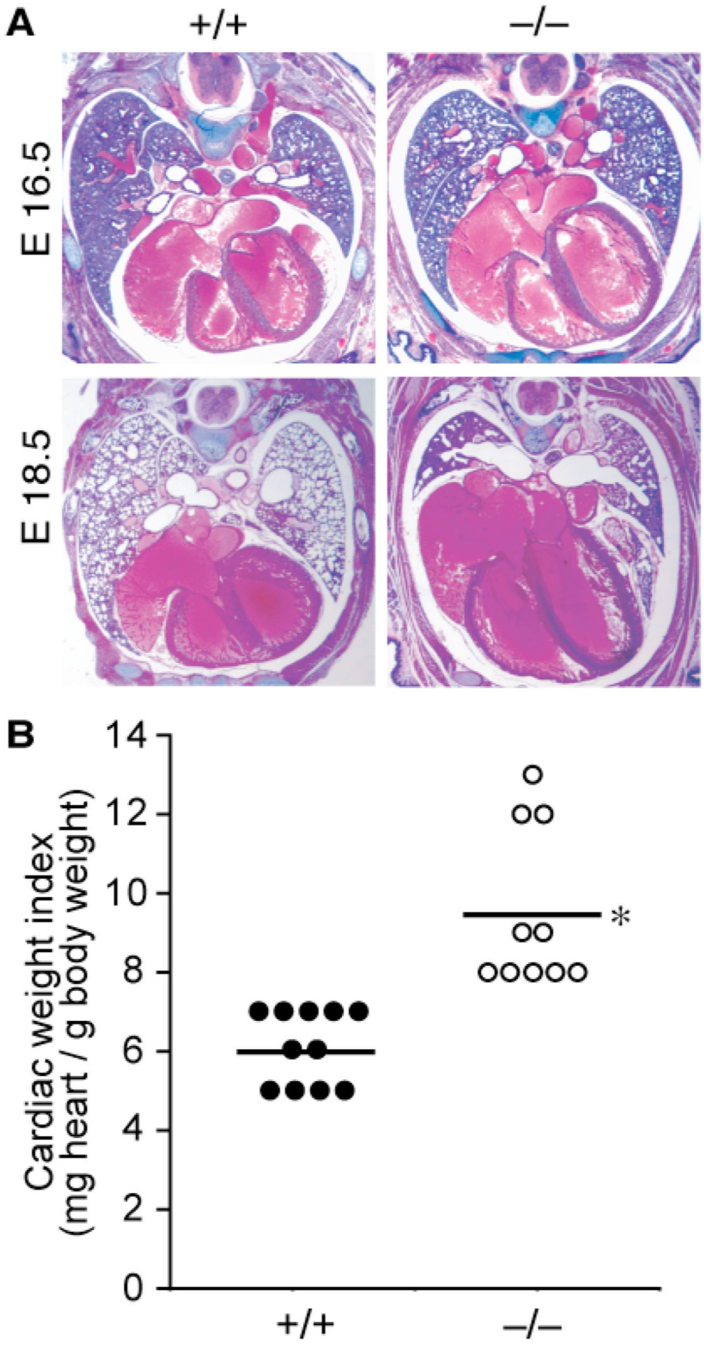

Figure 3.

Histopathology and cardiac weight index of Speg$^{-/-}$ embryos. (**A**) Cross-sections of Speg$^{+/+}$ (left panels) and Speg$^{-/-}$ (right panels) embryos of age 16.5 and 18.5 dpc were stained with H&E. Original magnification X20. (**B**) Cardiac weight index of wild type (+/+) and homozygous mutant (−/−) hearts. Hearts were harvested from 18.5 dpc embryos, and cardiac weight index (CWI) was calculated as heart weight (mg)/total body weight (g). The horizontal line in each column represents mean. *, $P<0.05$ versus Speg$^{+/+}$ hearts. n=10 in each group.

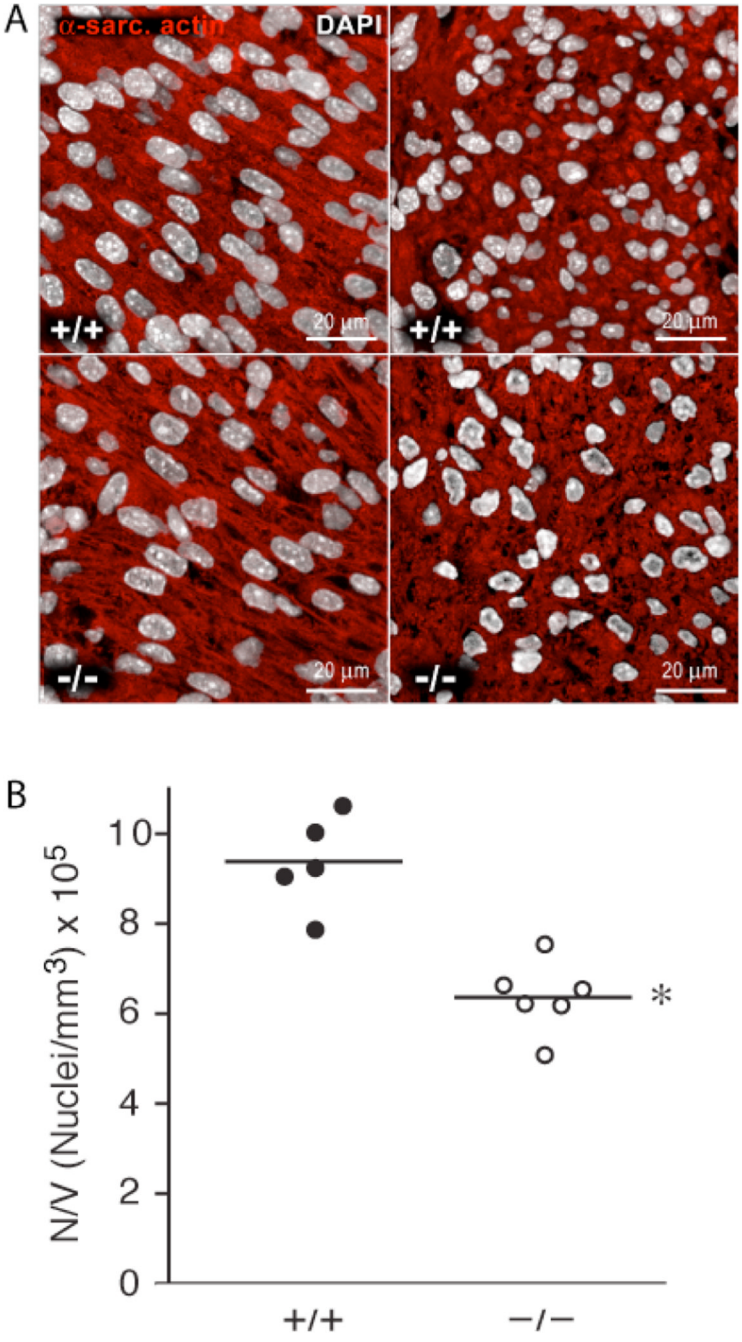

Figure 4.

Myocyte morphology in Speg$^{-/-}$ hearts. (A) Longitudinal (left panels) and transverse (right panels) sections of myocardium of Speg$^{+/+}$ and Speg$^{-/-}$ mice at 18.5 dpc. Myocytes were identified by α-sarcomeric actin (red). Nuclei were stained by DAPI (white). (B) Myocyte volume and number. The horizontal line in each column represents mean. *, $P<0.05$ versus Speg$^{+/+}$ hearts. Five Speg$^{+/+}$ and 6 Speg$^{-/-}$ mice were employed in this analysis. A total of 220 and 3,407 myocyte nuclei were measured in longitudinal and transverse sections of the myocardium, respectively.

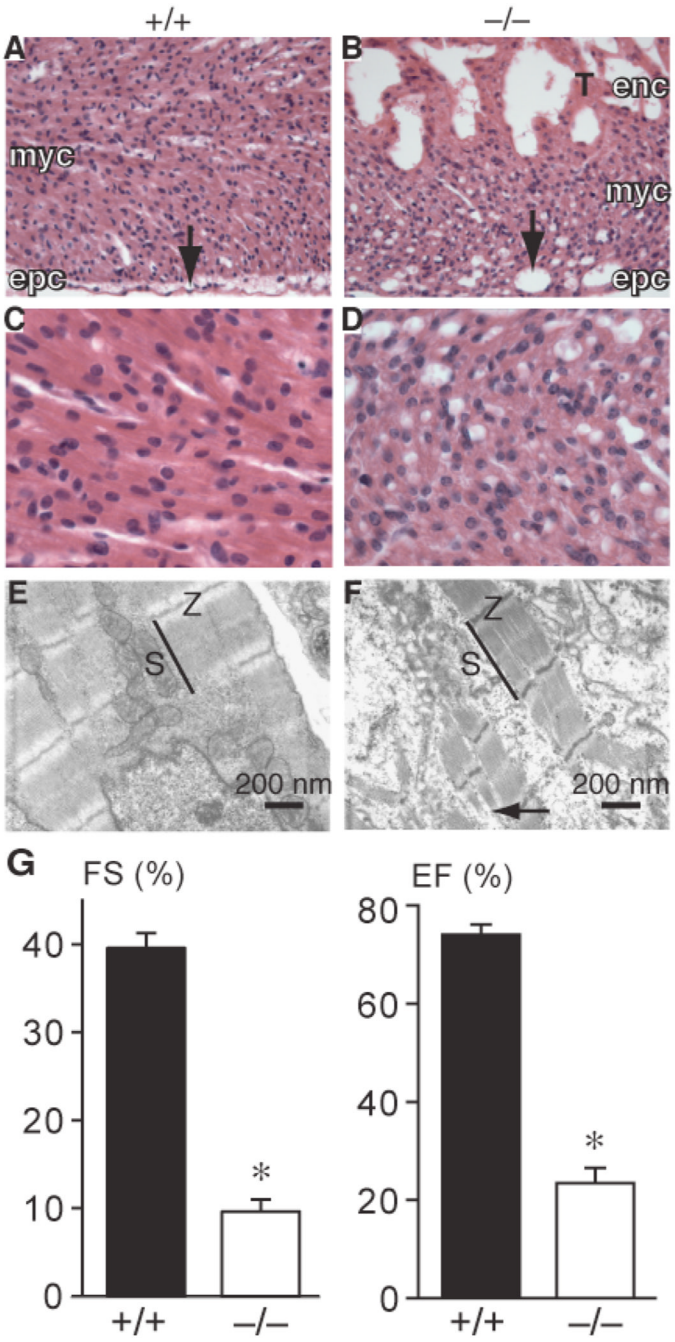

Figure 5.

Structural and functional defects in Speg$^{-/-}$ hearts. Panels **A–D** depict H&E staining of left ventricular free wall of Speg$^{+/+}$ (**A, C**) and Speg$^{-/-}$ (**B, D**) hearts from pups, postnatal day 1. Original magnification X200 (**A, B**) and X 400 (**C, D**). Myocardium (myc); endocardium (enc); epicardium (epc); trabeculae (T); arrow points to subepicardial vessels in panels **A** and **B**. Panels **E–F** show electron microscopy of Speg$^{+/+}$ (**E**) and Speg$^{-/-}$ (**F**) hearts of embryos 18.5 dpc. Sarcomere (S); and Z disc (Z). Arrow points to sarcomere fragmentation in panel **F**. (**G**) Echocardiograms were performed on 18.5 dpc Speg$^{+/+}$ (black bars, n=9) and Speg$^{-/-}$ (white bars, n=5) embryos. The left ventricles of hearts were assessed for fractional shortening (FS, %) and ejection fraction (EF, %). *, $P<0.05$ versus Speg$^{+/+}$ hearts.

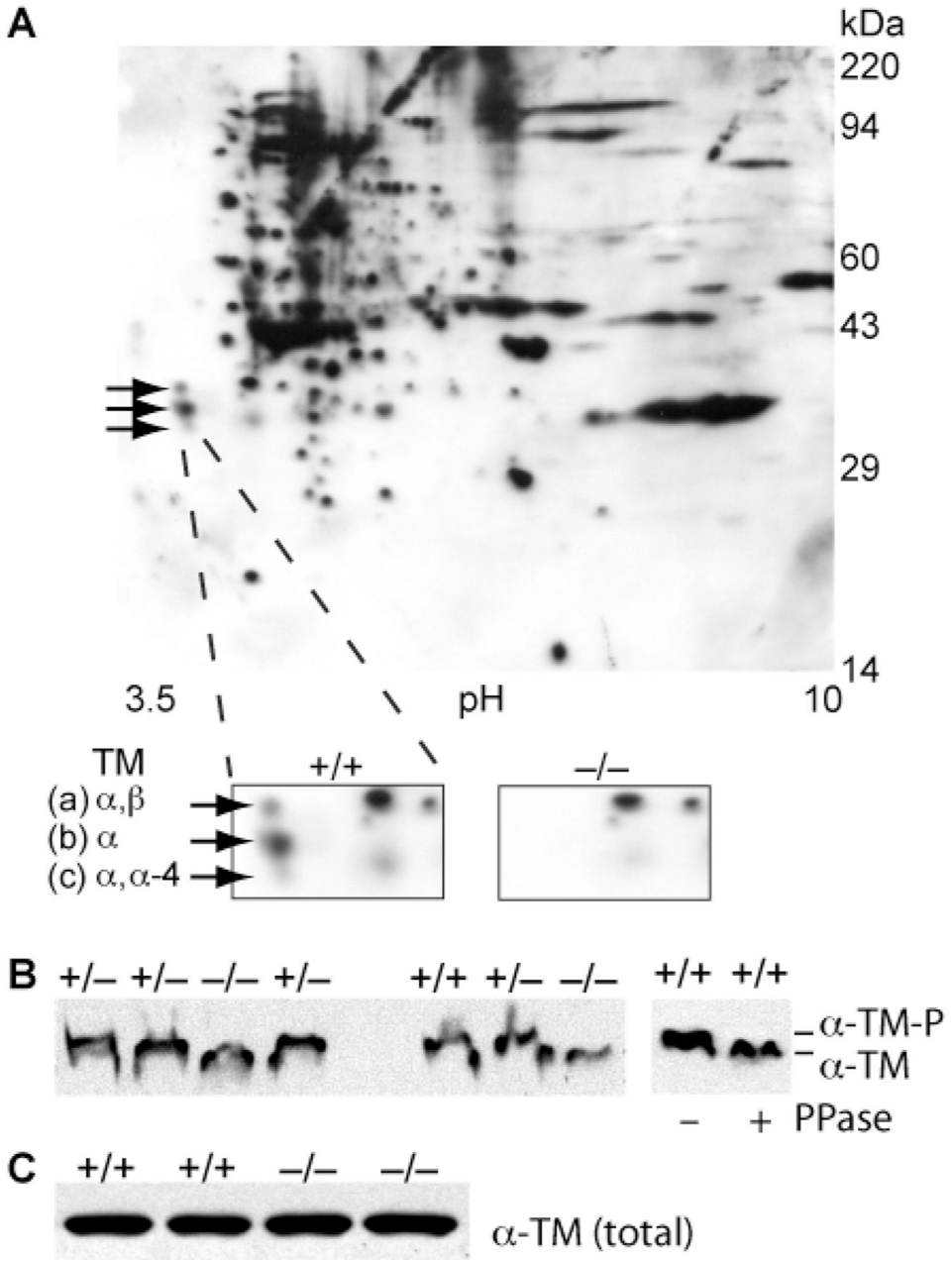

Figure 6.

Altered phosphorylation of tropomyosin (TM). (**A**) Protein (400 μg) extracted from 18.5 dpc Speg$^{+/+}$ and Speg$^{-/-}$ hearts was subjected to two-dimensional gel electrophoresis, followed by Western blotting with anti-serine/anti-threonine antibodies. Molecular mass markers are along the vertical axis, and pH gradient (3.5–10) along the horizontal axis. (**B**) Protein extracted from 16.5 dpc hearts was subjected to isoelectric focusing (IEF) electrophoresis, followed by Western blotting with an anti-tropomyosin antibody. Protein from Speg$^{+/+}$ hearts was also incubated in the presence (+) or absence (−) of phosphatase (PPase), and then IEF electrophoresis performed. (**C**) Conventional electrophoresis and Western blotting of protein from Speg$^{+/+}$ and Speg$^{-/-}$ hearts was performed using an anti-tropomyosin antibody.

Table 1

Mortality of Speg$^{-/-}$ Neonates

Age	n	+/+	+/−	−/−
11.5 – 15.5 dpc	122	26	53	21
18.5 dpc	175	21	58	21
Postnatal Day 1	105	24	53	23
Postnatal Day 2	25	36	60	4
Postnatal Day 21	360	29	69	2

Genotypes (%) of offspring from Speg$^{+/-}$ breeding at different gestational time points, and postnatal days 1, 2, and 21.